



ORIGINAL ARTICLE

Catalytic activity of Mn(III) porphyrin complex supported onto cross linked polymers in the green oxidation of malathion with hydrogen peroxide in aqueous solution



Sahar H. El-Khalafy^{a,*}, Mahmoud T. Hassanein^a, Samia M. Elsigeny^b,
Hazem F. Taha^a, Kamel R. Shoueir^c, El-Refaie S. Kenawy^d

^a Department of Chemistry, Faculty of Science, University of Tanta, Tanta 31527, Egypt

^b Department of Chemistry, Faculty of Science, Kafrelsheikh University, Kafrelsheikh 33516 Egypt

^c Institute of Nanoscience & Nanotechnology, Kafrelsheikh University, 33516 Kafrelsheikh, Egypt

^d Polymer Research Group, Department of Chemistry, Faculty of Science, University of Tanta, Tanta 31527, Egypt

Received 11 March 2023; accepted 27 April 2023

Available online 4 May 2023

KEYWORDS

Malathion. Metalloporphyrin;
Polymethyl methacrylate;
Poly(methyl methacrylate-co-styrene);
Catalytic oxidation

Abstract Developing effective, affordable, and recoverable heterogeneous catalysts is one of the foremost challenges in modern chemistry. Mn(III) complexes of 5-(4-aminophenyl)-10, 15, and 20-triphenyl porphyrin **1** immobilized covalently on polymethyl methacrylate (PMMA) **2** and poly(methyl methacrylate-co-styrene) (PMMA/ST) **3** were synthesized, characterized, and applied for degradation of malathion with H₂O₂ in aqueous solution. Mn(III) porphyrin complex anchored on cross linked polymers **4** and **5** show high catalytic activity for malathion (pesticide) degradation in an aqueous solution with green oxidant H₂O₂. The catalytic efficacy of malathion degradation was highest with the Mn(III) porphyrin complex covalently anchored on (polymethyl methacrylate-co-styrene) **5**. The optimum conditions, including the effect of pH, catalyst concentration, and H₂O₂ concentration on the degradation of malathion, were investigated. The reuse and stability of catalysts were examined, and the findings proposed that the Mn(III) porphyrin complex **5** has no noticeable changes in the removal efficiency up to five consecutive cycles. GC-MS analyses showed that the degraded compounds and intermediates formed from malathion degradation were non-toxic to *E. coli* bacteria. For the degradation of dissolved malathion pesticides in an aqueous

* Corresponding author.

E-mail address: sehar_hasouna@science.tanta.edu.eg (S.H. El-Khalafy).

Peer review under responsibility of King Saud University.



Production and hosting by Elsevier

solution, the use of Mn(III) porphyrin complex **5** in the presence of H₂O₂ has the potential to be advantageous.

© 2023 The Authors. Published by Elsevier B.V. on behalf of King Saud University. This is an open access article under the CC BY license (<http://creativecommons.org/licenses/by/4.0/>).

1. Introduction

Using chemical fertilizers and pesticides in agricultural processes is categorized as very harmful to the environment and human health (Ahmed et al., 2011; Kalyabina et al., 2021; Zaller et al., 2022). However, fertilizers and pesticides are used most for livestock and crop protection from insects, weeds, and pests (Bai et al., 2010; Fenner et al., 2013; Hassaan and El Nemr, 2020). Malathion [O,O-dimethyl-S-(1,2-dicarbethoxy)ethyl phosphorodithioate] is an organophosphorus insecticide widely used in agriculture to boost crop yield by reducing the negative impacts of insects and other pests. Most organophosphorus pesticides are highly toxic and act as potent inhibitors of acetylcholinesterase (AChE), a critical cholinergic enzyme that plays a vital role in neurotransmission by substituting acetylcholine (Kaushal et al., 2021; Rajagopalan et al., 2023). Malathion and its resultant byproducts in various environmental mediums such as soil, surface water, air, and groundwater have resulted in significant contamination. This contamination has been found to have adverse effects on aquatic life (Vormeier et al., 2023) and other living organisms (Juraska et al., 2007; Sarangapani et al., 2016) due to the high levels of toxicity associated with these substances.

Presently, diverse techniques are employed to eliminate particular residual pesticides from water and soil. Several methods have been employed to reduce emerging contaminants (ECs) concentrations in water. These methods include biodegradation, sand filtration, microfiltration, membrane bioreactor, plant-microorganism combined technology, and activated carbon adsorption (Parida et al., 2021). However, it has been observed that these methods are inadequate in achieving the desired reduction of ECs during water treatment, as per the permissible limits (Lafi and Al-Qodah, 2006; Malakootian et al., 2020).

The highly efficient and novel method with the ability to break down toxic pesticides into less harmful by-products is the advanced oxidation process (AOPs). Several techniques have been approved for the degradation of different types of pesticides from aqueous systems, such as ozone (Pandiselvam et al., 2020), the Fenton process (Pandiselvam et al., 2020), adsorption (T. Wang et al., 2020), plasma (Liu et al., 2021), and metalloporphyrins (Lage et al., 2019; Martins et al., 2022; Rebelo et al., 2009).

Metalloporphyrin has been utilized as a biomimetic catalyst for Cytochrome P450 enzymes and has demonstrated successful outcomes in various oxidation reactions (Lage et al., 2019). Metalloporphyrin stability has been enhanced through their integration into solid substrates, including but not limited to zeolites, silica, clays, ion-exchange materials, carbonaceous substances, and metal oxides (Ema et al., 2013; Ghafuri et al., 2016). This integration is accomplished through covalent, van der Waals, or electrovalent bonding mechanisms.

Unlike the above compound, heterogeneous metalloporphyrins immobilized on cross linked polymers are promising and challenging due to good catalytic activity and reusability. A limited number of literature is available on the breakdown of malathion through advanced oxidation processes (AOPs). Tony et al. (Tony et al., 2017) examined the degradation of malathion by chemical oxidation employing (NaOCl, Ca(OCl)₂, monochloride-isocyanuric acid (MCICA), dichloro *iso*-cyanuric acid (DCICA), and trichloroisocyanuric acid (TCICA), UV, and ozone in simulated wastewater. They discovered that TCICA should be employed since it was more efficient than other chlorinating materials, yielding a breakdown of malathion of 47.0% after 12 h.

The prior literature review suggests that implementing the AOP is an appropriate approach for the remediation of pesticide-contaminated wastewater. However, the impact of the process parameters on performance effectiveness is poorly understood (Pérez et al., 2006). This study examines the degradation of malathion to environmentally less objectionable substances using the heterogeneous catalyst Mn(III) complex of 5-(4-Aminophenyl) -10, 15, 20-triphenylporphyrin **1** covalently immobilized on cross linked polymethyl methacrylate (PMMA) **2** and poly(methyl methacrylate-co-styrene) (PMMA/ST) **3**. To the best of our knowledge, this is the first report on the degradation of malathion in an aqueous solution by Manganese (III) porphyrin complex supported on cross linked polymers.

2. Experimental

2.1. Materials and methods

Methyl methacrylate (99%, stabilized, CH₂ = C(CH₃)COOCH₃), styrene (analytical standard, C₆H₅CH = CH₂), and divinylbenzene technical grade, (80% C₆H₄(CH = CH₂)₂), sodium nitrite (NaNO₂, ACS, 97%), trifluoroacetic acid (CF₃-COOH), Tetra-n-butylammonium bromide, TBAB ((CH₃-CH₂CH₂CH₂)₄NBr) were supplied from Sigma Aldrich. Merck provided pyrrole (pH > 6 (10 g/l, H₂O, 20 °C)) and benzaldehyde. Malathion was delivered from Accustandard, USA. All solvents and acids were supported from Loba Chemie.

2.2. Characterization

UV/visible measurements were conducted using a Perkin-Elmer Lambda 35 spectrophotometer.

FTIR studies were carried out on A JASCOFT/IR 6800 instrument.

¹H NMR spectra were measured on a Bruker AC-200 spectrometer.

GC/MS measured on Varian GC model CP3800 and Mass model 320x.

The Perkin Elmer 3100 Atomic Absorption Spectrometer (AAS) was employed to detect manganese concentration.

The Mn(III)porphyrin complex morphologies with PMMA and PMMA/ST were characterized using a scanning electron microscope (SEM, Joel, JSM-6510LV, Japan).

2.3. Preparation of catalyst

2.3.1. Preparation of Mn(III) complex of 5-(4-Aminophenyl) -10, 15, 20-triphenyl porphyrin **1**

The free base porphyrin 5-(4-Aminophenyl) -10, 15, 20-triphenylporphyrin, and the corresponding Mn(III) porphyrin complex **1** was produced and purified using a previously known technique (Adler et al., 1970; Luguva et al., 2004).

Sodium nitrite (100 mg, 1.45 mmol) was added to tetra phenyl porphyrin (500 mg, 0.815 mmol) dissolved in trifluo-

roacetic acid (50 mL). The mixture was stirred at room temperature for 3 min, then poured into 100 mL of water and extracted with dichloromethane four times. The organic layer collected was rinsed numerous times with saturated aqueous NaHCO_3 and water, and the solvent was then drawn out under a vacuum. The residue (5-(4-Nitrophenyl) -10, 15, 20-triphenylporphyrin) obtained was dissolved in 50 mL concentrated HCl, and tin (II) chloride (1.1 g, 0.975 mmol) was added carefully while stirring, heated to 65 °C for 1 h under nitrogen, and then poured into 500 mL of cold water. The pH was adjusted to 8 using an ammonium solution, and dichloromethane was used to extract the aqueous solution until it was colorless. The organic layer obtained evaporated under vacuum, and the final residue recrystallized from methanol, yielding 410 mg (82%) of 5-(4-Aminophenyl) -10, 15, 20-triphenylporphyrin.

^1H NMR (CDCl_3) δ ppm: -2.82(2H, s, inner NH), 4.14 (8H, s, Ph-NH₂), 6.96 (2H, d, ArH), 7.672 (9H, m, ArH), 7.89 (2H, d, ArH), 8.13 (6H, m, ArH), 8.84 (8H, s, pyrrole- β CH). UV-Vis (CHCl_3) λ_{max} : 417, 514, 551, 589, and 645.

Mn(III) porphyrin complex **1** was obtained by refluxing 5-(4-Aminophenyl) -10, 15, 20-triphenyl porphyrin (200 mg, 0.32 mmol) with Manganese (II) Acetate (624 mg, 3.2 mmol) in 70 mL of N, N-dimethylformamide for 3 h. The solution was cooled at room temperature under stirring. DMF was removed by distillation under a vacuum and washed with distilled water. Then the residue was dissolved in 20 mL of CHCl_3 and filtered to get rid of impurities. The solvent was removed under vacuum, and a dark-green solid of Mn(III)porphyrin complex **1** was obtained (Adler et al., 1970). The sorbent band of the dark-green solid **1** obtained after the metal insertion reaction was 479 nm in CHCl_3 instead of 417 nm of the free base.

2.3.2. Synthesis of cross linked poly methyl methacrylate (PMMA) and its copolymer with styrene (PMMA/ST)

Poly methyl methacrylate (PMMA) **2** and its copolymer with styrene (PMMA/ST) **3** (Fig S1) were synthesized following a

previously reported procedure (Akelah et al., 1986) to form two types of supported polymer, polymethyl methacrylate PMMA **2** and PMMA/ST **3**.

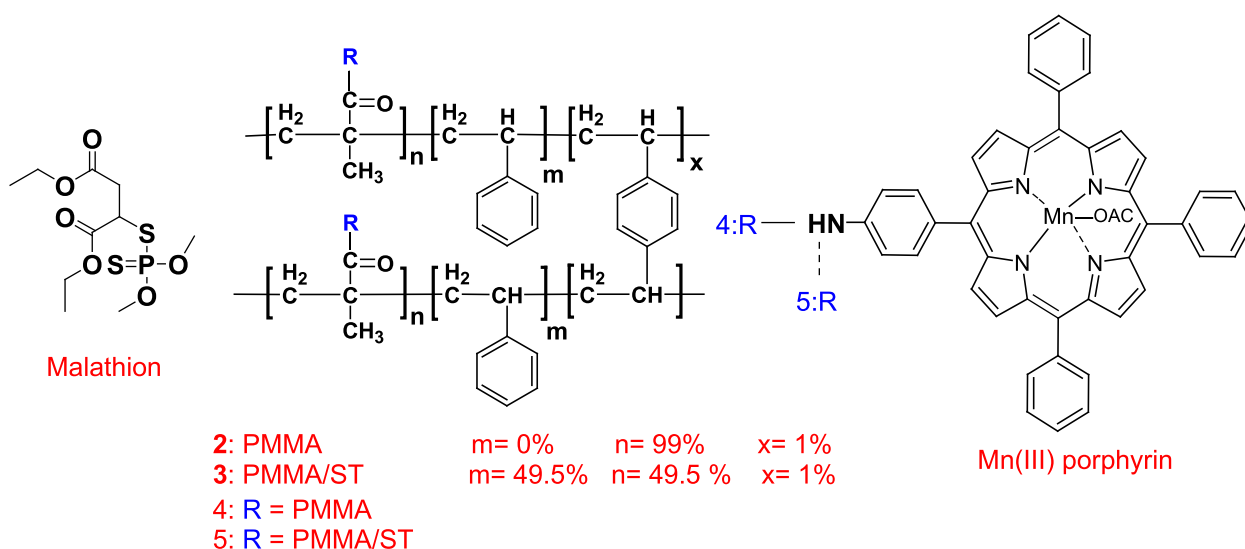
2.3.3. Synthesis of Mn(III) porphyrin complex 1 supported on cross linked polymers (2,3)

A 0.5 g of polymers, PMMA **2** or PMMA/ST **3**, and 40 mg of Mn(III) porphyrin complex **1** were added to 20 mL of DMF and 0.3 g (10 mmol) tetra-n-butyl ammonium bromide (TBAB) as catalyst was stirred at 100 °C for 2 days. The resins were obtained by filtration, washed with water and methanol, and dried under a vacuum (Scheme 1) yielding 92% of Mn(III) complex immobilized covalently on polymethyl methacrylate **4** and 88% of Mn(III) complex immobilized covalently on (polymethyl methacrylate-co-styrene) **5**. Using atomic absorption spectroscopy (AAS), the Mn content determined for resins (**4**, **5**) were 2.68 and 1.85 mg, respectively.

2.4. Catalyzed degradation of malathion by Mn(III) porphyrin complex supported on cross linked polymer (4 & 5) by H_2O_2

Oxidation degradation of malathion catalyzed by Mn(III) porphyrin complex supported on cross linked polymer (**4** & **5**) by H_2O_2 was carried out as the following method. A 50 mL aliquot of deionized water was placed in a 100 mL Erlenmeyer flask. A 20 μL aliquot of 0.01 M malathion in methanol and 50 mg of catalyst were added to the solution. The oxidative reaction was initiated by adding 100 μL aliquot of 1 mM aqueous solution of H_2O_2 under stirring at 150 rpm at room temperature. An aliquot was withdrawn at regular intervals, and the remaining malathion concentrations were measured using a GC - NPD detector with the standard method (EPA method 507) (Moriya et al., 1983).

The degradation rate constant (k_{obs}) of malathion was estimated by applying the least-square approximation method to the equation $C/C_i = \exp(-kt)$, where C and C_i are pesticides concentration at time t (in min) and t = 0, respectively.



Scheme 1 Structure configuration of malathion, PMMA, PMMA/ST, and Mn(III)porphyrin.

2.5. Recovery and reuse of supported Mn(III) porphyrin complexes

The cross linked polymers supported by Mn(III)porphyrin complex (**4,5**) were reused from the reaction mixture by simple filtration, washing the catalyst with distilled water several times, and then recycled for subsequent experiments.

2.6. Toxicity assay

The study employed the reduction assay technique to assess the toxicity of malathion degradation products, utilizing the Gram-negative *Escherichia coli* strain (ATCC25922). The utilization of the resazurin dye reduction assay is a widely recognized method for assessing the toxicity of various chemical substances. A suspension of *E. coli* strain cells at a concentration of 10^5 /mL was prepared in 10 mL of sterile saline solution (Li et al., 2019).

The toxicity of the bacterial culture *E. coli* was assessed by preparing reagent control, cell control, and chemical test in 2 mL vials. These vials contained 1 mL of the growth medium, composed of 2.64 g of K_2HPO_4 , 1.64 g of KH_2PO_4 , 0.2 g of glucose, 0.2 g of sodium acetate, and 1.6 g of nutrient broth dissolved in 1 L of distilled water. Additionally, 250 μ L of resazurin dye solution (10 μ g/mL) was added to each vial. For the cell control and chemical test, 250 μ L of bacterial cells saline solution was also added.

2.7. Degradation experiments

The process of malathion degradation was executed by introducing 100 μ L of byproducts into chemical test vials at per-hour intervals, followed by incubation of all vials at 37 °C for 4 h. Upon reduction, the resazurin dye changed from blue to pink. The dye reduction process was assessed by employing a Spectrophotometer at a wavelength of 610 nm after the elimination of bacterial cells via centrifugation. The quantification of the chemical examination toxicity on the bacterial culture was determined by calculating the percentage inhibition of the dehydrogenase activity, as per the provided equation:

$$Inh.(%) = (C - B)/(A - B) \times 100 \quad (1)$$

Inh. (%) = percent inhibition at a given time, A = final absorbance of the reagent control, B = final absorbance of the cell control, and C = final absorbance of the chemical test.

3. Results and discussion

3.1. Structural and morphological characteristics

Using heterogeneous catalysis to create practical and environmentally friendly synthetic techniques to break down pesticides is quite interesting. Using the newly developed metalloporphyrin immobilized on cross linked polymer as an ecologically safe solid-supported catalyst with high catalytic activity under benign conditions, malathion can be degraded effectively, conveniently, and practically.

To verify the covalent interactions between Mn(III) porphyrin complex **1** immobilized on cross linked polymers (**2,3**), FTIR spectra were recorded for PMMA **2**. (Fig S2.a) shows a sharp, intense peak at 1735 cm^{-1} , indicating the pres-

ence of ester carbonyl group stretching vibration. The broad peak appears from $1252\text{ to }997\text{ cm}^{-1}$ due to the stretching vibration of the C-O (ester bond). The broadband from $846\text{ to }702\text{ cm}^{-1}$ is due to the bending of C-H. Bands of the FT-IR spectrum for polystyrene in PMMA/ST **3** (Fig S3.a) according to their functional groups, C-H aromatic tension appear from $3089\text{ cm}^{-1} - 3016\text{ cm}^{-1}$, 2929 cm^{-1} and 2842 cm^{-1} CH_2 asymmetric and symmetric tension; $1951 - 1799\text{ cm}^{-1}$, aromatic ring mono substitution; 1449 cm^{-1} deformation $\text{CH}_2 + \text{C} = \text{C}$ of the aromatic ring.

The present study investigates the main functional properties of Mn(III)porphyrin complex/ PMMA **4** and Mn(III)porphyrin complex (PMMA/ ST) **5**. Upon loading Mn(III) porphyrin complex onto PMMA **2** and PMMA/ST **3**, the FT-IR spectrum exhibited the emergence of bands at 1664 cm^{-1} , indicative of N-H bending vibration, and 1268 cm^{-1} , indicative of C-N stretching vibration (Fig S2.b & Fig S3.b).

SEM examined the surface texture of catalysts **4** and **5**. The copolymer composition affects the matrix morphology, as shown in Fig. 1. Pure PMMA surface is rough due to the formation of sticky layers Fig. 1a. The morphology was changed with PMMA/ST copolymer Fig. 1b, and the structure consisting of rigid sheets is well-distributed and well-wetted in the matrix. When Mn(III)porphyrin complex was doped on the surface of PMMA (Fig. 1c) and PMMA/ST (Fig. 1d), there was no clustering of the sheet fillers observed. The presence of metal-centered porphyrin totally affected the distribution of nanoparticles (Zhang et al., 2022). The nanoparticles are spherical with an average SEM diameter of $53 \pm 9\text{ nm}$ and $61 \pm 10\text{ nm}$ for the Mn(III)porphyrin complex with PMMA and crosslinked PMMA/ST, respectively. The nanoparticles formation and distribution were dependent on surface modification, polar groups, and covalent interaction.

3.2. Catalytic degradation of malathion

In this section, the catalytic activity of the synthesized Mn(III) porphyrin complex supported on cross linked polymers (**4,5**) was studied for degradation of malathion, as a model of organic water pollutants, in the presence of H_2O_2 . As shown in Fig. 2, malathion was persistent and stable in the presence of PMMA **2** and PMMA/ST **3** without any catalyst. Only about 10 % of adsorption occurs in PMMA **2** and 5% in the case of PMMA/ST **3**. The poor removal ratio may be attributed to the aggregation of ST on the surface of PMMA and their hydrophobic nature (M. Wang et al., 2020). Otherwise, in the presence of pure H_2O_2 and without any catalyst, 40% degradation occurs for malathion.

The homogeneous catalysis of Mn(III) porphyrin complex **1** in the presence of H_2O_2 was also carried out. It can be seen that 85% of malathion was degradable due to the activation of the Mn(III) porphyrin complex to form high valent oxo complexes Mn(V)-oxo complexes using hydrogen peroxide which was reported previously in similar systems as shown in equations (2)&(3) (Procner et al., 2020, 2016; Saha et al., 2013). Exposure of malathion to an H_2O_2 -based oxidant supported on cross-linked polymers **4** and **5** resulted in a steady increase in degradation of malathion, with approximately 94% and 100% of the target substrate, respectively. The results demonstrated that both catalysts supported on polymers **4** and **5**

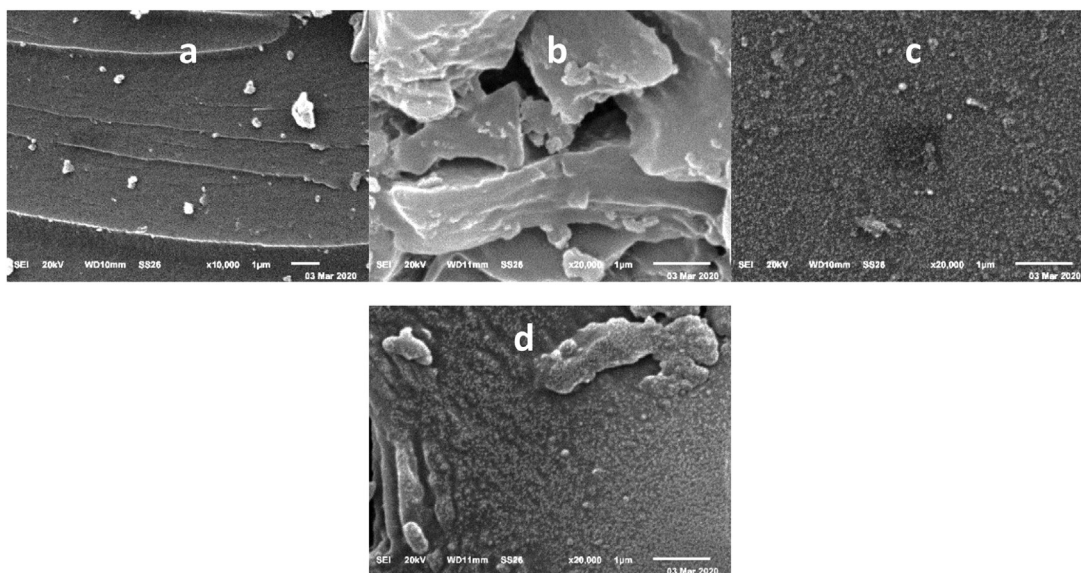


Fig. 1 SEM Images for (a) PMMA, (b) PMMA/ST copolymer, (c) Mn(III)porphyrin complex /PMMA, and (d) Mn(III)porphyrin complex /PMMA/ST copolymer.

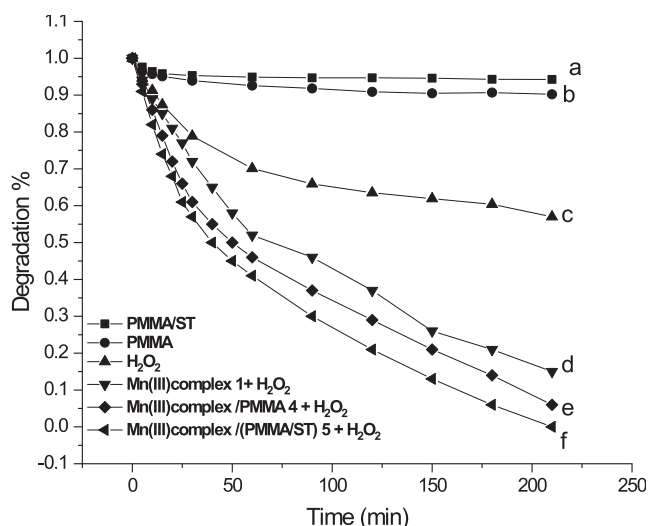
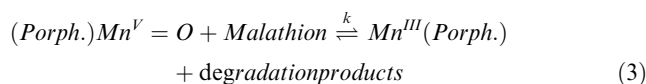


Fig. 2 The degradation of Malathion (initial concentration 10 mg/L(30.27 μ M) 50 mL, pH = 7, T = 25°C) under various systems: (a) PMMA/ST (0.1 gm); (b) PMMA (0.1 g); (c) substrate + H₂O₂ (1 mM), (d) Mn(III) porphyrin complex 1 (35 μ M) and H₂O₂ (1 mM); (e) Mn(III) porphyrin complex / PMMA 4 (0.07 g, containing 35 μ M of Mn(III) complex 1 and H₂O₂ (1 mM); (f) Mn(III) porphyrin complex (PMMA/ ST) 5 (0.1 g, containing 35 μ M of Mn(III) complex 1)and H₂O₂ (1 mM).

show high catalytic activity for malathion degradation. However, the most increased degradation was observed for the Mn(III)porphyrin complex supported on poly(methyl methacrylate-co-styrene) **5**. This finding might be attributed to the presence of a polystyrene hydrophobic block which is immobilized onto the complex. Consequently, the distributed **5** onto the surface of the complex exhibits a high photoreponse in the visible range boosting its catalytic activity.



As shown in Fig. 2, Mn(III) porphyrin complex / (PMMA/ ST) **5** has been selected to optimize the experimental conditions for malathion degradation.

3.2.1. Effect of pH on degradation of malathion

Malathion degradation was investigated within the pH range of 5 to 9, as depicted in Fig. 3. Data illustrated in Fig. 3 show that malathion degradation increased with increasing pH of the reaction mixture from 5.0 to 9.0. Thus, the effect of pH on the degradation of malathion is apparent. The higher the pH of the solution, the faster the degradation of malathion due to the more efficient generation of the active form of the catalytic species owing to the much higher reactivity of OOH⁻ than H₂O₂. This results in agreement with the work previously published (Jin et al., 2010).

3.2.2. Effect of catalyst concentration on the rate of malathion degradation

At various concentrations of Mn(III) porphyrin complex/ (PMMA/ST) **5** at fixed [H₂O₂] and [malathion], the impact of the catalyst concentration on the degradation of malathion was investigated. The data in Fig. 4 indicate that the rate constant, k_{obs}, exhibits a pseudo-first-order behavior and increases proportionally with catalyst employed. A plateau is observed when a substantial amount of Mn(III) porphyrin complex / (PMMA/ ST) **5** was utilized (Silva et al., 2010).

3.2.3. Effect of hydrogen peroxide concentration

In the concentration range of 0.05 mM to 3 mM, the impact of H₂O₂ concentration on the breakdown of malathion was studied. Fig. 5 demonstrates that the degradation rate exhibits an upward trend as the concentration of H₂O₂ is elevated from 0.05 mM to 1 mM. The total degradation process is not accel-

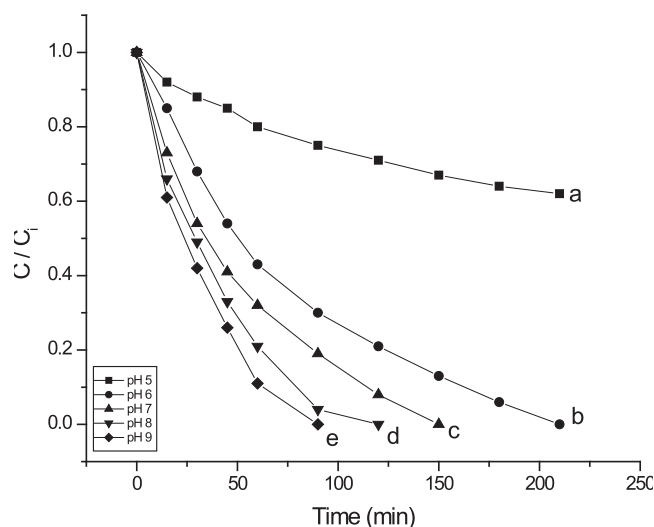


Fig. 3 Effect of pH on malathion degradation (initial concentration 10 mg/L (30.27 μ M), H_2O_2 (1 mM), $T = 25^\circ\text{C}$) in the presence of Mn(III) porphyrin complex (PMMA/ ST) **5** (0.14 g, containing 50 μ M of Mn(III) complex 1) at (a) pH 5, (b) pH 6, (c) pH 7, (d) pH 8 and (e) pH 9. The pH was adjusted to 5 using a sodium acetate and acetic acid buffer mixture, and the pH was adjusted to 6 using a sodium citrate buffer mixture. pH 7 and 8 were adjusted using potassium dihydrogen phosphate, disodium hydrogen phosphate, and pH 9 using a borax and HCl buffer mixture.

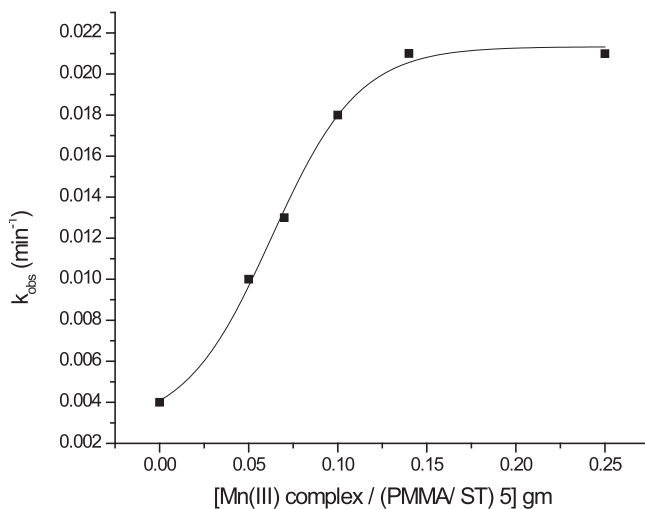


Fig. 4 Dependence of k_{obs} on the concentration of Mn(III) complex / (PMMA/ ST) **5** for malathion degradation (initial concentration malathion 10 mg/L (30.27 μ M), H_2O_2 (1 mM), pH = 7 and $T = 25^\circ\text{C}$).

erated by an additional increase in H_2O_2 concentration, which establishes the rate at which the catalyst partially decomposes (Trocha et al., 2021).

3.2.4. Recovery and reuse for polymers supported Mn (III) complex 4 and 5 for malathion degradation

The Mn(III) complex supported on polymers 4 and 5 was easily recycled from the reaction media by straightforward filtration, rinsed numerous times with water, and utilized for

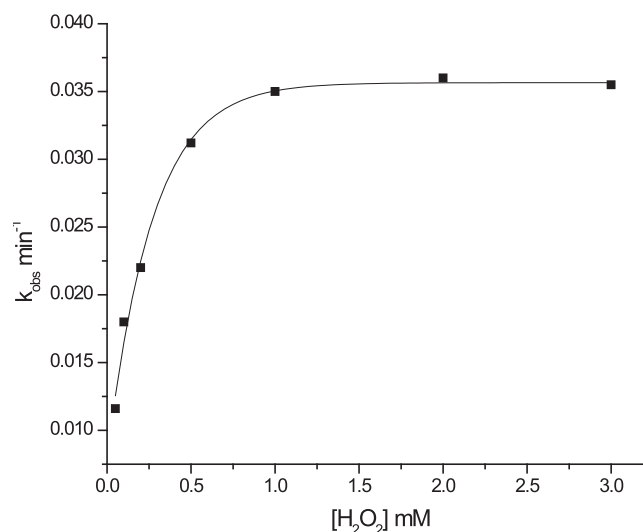


Fig. 5 Dependence of k_{obs} on total H_2O_2 concentration for degradation of malathion by **5**. ([malathion] = 10 mg/L (30.27 μ M), Mn(III) porphyrin complex (PMMA/ ST) **5** (0.14 g, containing 50 μ M of Mn(III) complex 1), pH = 7 and $T = 25^\circ\text{C}$).

subsequent experiments. The proportion of malathion degradation after five consecutive runs was shown in Fig. 6. The recycled Mn(III) porphyrin complex supported on PMMA – co-ST **5** has great catalytic stability. It exhibits no notable alterations until the third run (losses of 8%), as opposed to the Mn(III) complex supported on PMMA **4** (losses of 20%).

According to these findings, the Mn(III) complex supported on polymer **5** can be used again for the following degrading experiment since PMMA/ST was securely fixed on the complex (Fang et al., 2020).

3.2.5. Identification of the degradation products

The identification of the malathion degradation products catalyzed by the Mn(III) complex/(PMMA/ST) **5** with H_2O_2 by

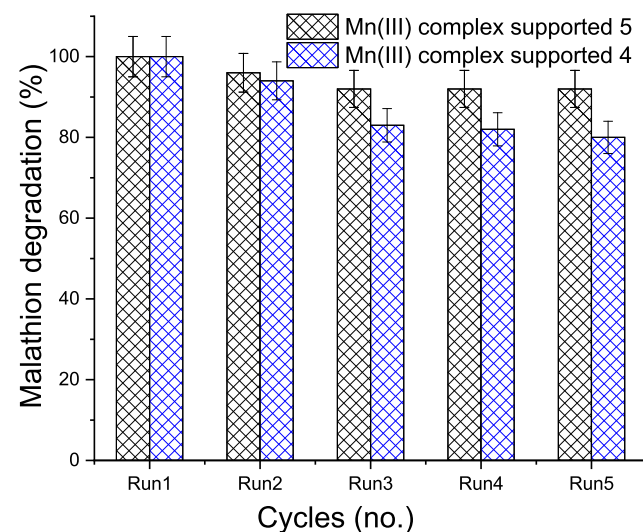
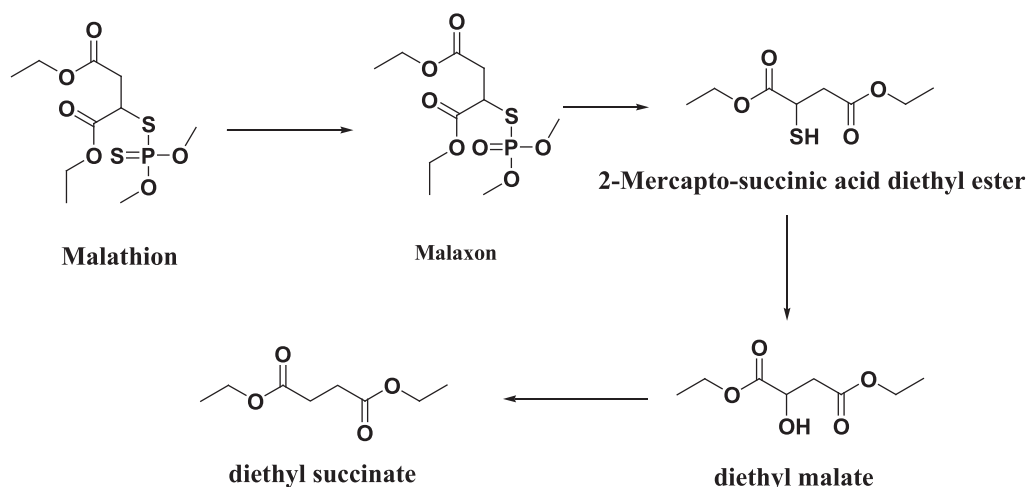


Fig. 6 Recycle of catalyst **4** & **5** for degradation of malathion ([malathion] = 10 mg/L (30.27 μ M), 50 μ M Mn(III) complex, H_2O_2 (1 mM), pH = 7 and $T = 25^\circ\text{C}$) after 210 min.



Scheme 2 The outline scheme depicts the potential pathways of malathion degradation.

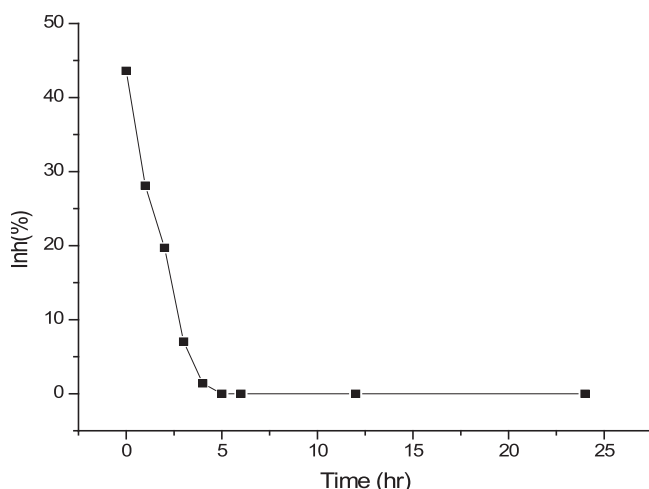


Fig. 7 Effect of malathion degradation product on inhibition of *E. coli* bacteria with time.

GC/MS (Scheme 2) reveals that the main products observed were malaxon (m/z 314), 2-mercapto-succinic acid diethyl ester with (m/z 206), diethyl malate (m/z 190) and diethyl succinate (m/z 174), which were also agreement with published elsewhere (Kaur et al., 1997; Tony et al., 2017).

3.2.6. Bacterial toxicity of degradation products

The resazurin dye reduction assay successfully estimates the toxicity assays for a wide range of toxic chemicals (Brouwer, 1991; Chung et al., 2013; Eker and Kargi, 2009; Strotmann and Eglsaer, 1995). In the presence of an active bacterial culture of *E. coli*, the resazurin changes color from blue to pink. If bacterial growth is inhibited, resazurin reduction does not occur, and a sample does not alter its blue color. If the products of malathion degradation on the chemical test have no inhibition effect, then the resazurin is reduced to the pink color. Fig. 7 shows the impact of the malathion degradation product on the inhibition of *E. coli* bacteria with time. A high percentage of inhibition was observed at the beginning of the degradation of malathion with H_2O_2 catalyzed by Mn(III)

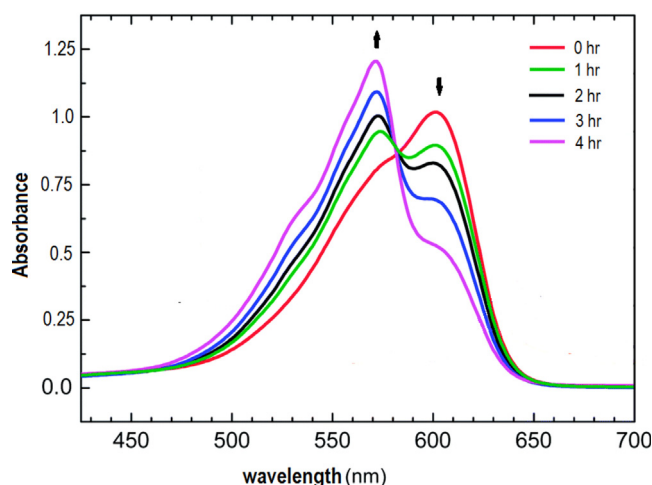


Fig. 8 Changes in UV-VIS spectra of resazurin dye reduction assay for malathion degradation products during the degradation interval times.

complex / (PMMA/ ST) **5**. Then the inhibition percent decreased with increasing degradation time till it reached zero inhibition after completing the degradation of malathion, and the cell transformed to pink, similar to the control with only *E. coli*. Fig. 8 illustrates the transformation of the resazurin dye from blue to pink as a result of the degradation of malathion using Mn(III) complex / (PMMA/ ST) **5** over time in the presence of H_2O_2 . The findings suggest that the degradation products of malathion do not exhibit any inhibitory effects, thereby indicating their non-toxicity towards bacteria.

4. Conclusion

Mn(III) porphyrin complex anchored on cross linked polymers **4** and **5** show high catalytic activity for degradation of malathion in an aqueous solution with green oxidant H_2O_2 . The rate constant for malathion degradation was found to increase with increasing the pH of the reaction medium, catalyst concentration, and initial concentrations of H_2O_2 .

Mn(III) porphyrin complex immobilizing on polymethyl methacrylate-co-styrene **5** showed high stability and no significant changes till the five runs. GC/MS showed that some leading products are utilized in corrosion inhibitors, electroplating agents, and active pharmaceutical ingredients.

Malathion degradation products are non-toxic to bacteria, and the blue color of resazurin dye is wholly reduced to pink color after five hours of degradation.

Declaration of Competing Interest

The authors declare that they have no known competing financial interests or personal relationships that could have appeared to influence the work reported in this paper.

Appendix A. Supplementary material

Supplementary data to this article can be found online at <https://doi.org/10.1016/j.arabjc.2023.104969>.

References

- Adler, A.D., Longo, F.R., Kampas, F., Kim, J., 1970. On the preparation of metalloporphyrins. *J. Inorg. Nucl. Chem.* 32, 2443–2445.
- Ahmed, S., Rasul, M.G., Brown, R., Hashib, M.A., 2011. Influence of parameters on the heterogeneous photocatalytic degradation of pesticides and phenolic contaminants in wastewater: a short review. *J. Environ. Manage.* 92, 311–330.
- Akelah, A., Hassanein, M., Selim, A., Kenawy, E.-R., 1986. Synthesis and chemical modification of poly (methyl methacrylate) resins. *Eur. Polym. J.* 22, 983–985.
- Bai, Y., Chen, J., Yang, Y., Guo, L., Zhang, C., 2010. Degradation of organophosphorus pesticide induced by oxygen plasma: effects of operating parameters and reaction mechanisms. *Chemosphere* 81, 408–414.
- Brouwer, H., 1991. Testing for chemical toxicity using bacteria: an undergraduate laboratory experiment. *J. Chem. Educ.* 68, 695.
- Chung, S.-G., Chang, Y.-S., Choi, J.-W., Baek, K.-Y., Hong, S.-W., Yun, S.-T., Lee, S.-H., 2013. Photocatalytic degradation of chlorophenols using star block copolymers: removal efficiency, by-products and toxicity of catalyst. *Chem. Eng. J.* 215, 921–928.
- Eker, S., Kargi, F., 2009. Biological treatment of 2, 4, 6-trichlorophenol (TCP) containing wastewater in a hybrid bioreactor system with effluent recycle. *J. Environ. Manage.* 90, 692–698.
- Ema, T., Miyazaki, Y., Taniguchi, T., Takada, J., 2013. Robust porphyrin catalysts immobilized on biogenous iron oxide for the repetitive conversions of epoxides and CO₂ into cyclic carbonates. *Green Chem.* 15, 2485–2492.
- Fang, H., Wang, M., Yi, H., Zhang, Y., Li, X., Yan, F., Zhang, L., 2020. Electrostatic assembly of porphyrin-functionalized porous membrane toward biomimetic photocatalytic degradation dyes. *ACS Omega* 5, 8707–8720.
- Fenner, K., Canonica, S., Wackett, L.P., Elsner, M., 2013. Evaluating pesticide degradation in the environment: blind spots and emerging opportunities. *Science* 341, 752–758.
- Ghafari, H., Rahmani, S., Rahimi, R., Mohammadiyan, E., 2016. Synthesis and characterization of benzilic alcohol metalloporphyrin and its nanocomposite with graphene oxide (GO–CoTHMP) and investigation of their efficiency in the removal of environmental pollutants. *RSC Adv.* 6, 62916–62922.
- Hassaan, M.A., El Nembr, A., 2020. Pesticides pollution: classifications, human health impact, extraction and treatment techniques. *Egypt. J. Aquat. Res.* 46, 207–220.
- Jin, N., Lahaye, D.E., Groves, J.T., 2010. A “Push– Pull” Mechanism for Heterolytic O– O Bond Cleavage in Hydroperoxo Manganese Porphyrins. *Inorg. Chem.* 49, 11516–11524.
- Juraske, R., Antón, A., Castells, F., Huijbregts, M.A.J., 2007. Human intake fractions of pesticides via greenhouse tomato consumption: comparing model estimates with measurements for Captan. *Chemosphere* 67, 1102–1107.
- Kalyabina, V.P., Esimbekova, E.N., Kopylova, K.V., Kratasyuk, V. A., 2021. Pesticides: formulants, distribution pathways and effects on human health—a review. *Toxicol. Rep.* 8, 1179–1192.
- Kaur, I., Mathur, R.P., Tandom, S.N., Dureja, P., 1997. Identification of metabolites of malathion in plant, water and soil by GC–MS. *Biomed. Chromatogr.* 11, 352–355.
- Kaushal, J., Khatri, M., Arya, S.K., 2021. A treatise on Organophosphate pesticide pollution: current strategies and advancements in their environmental degradation and elimination. *Ecotoxicol. Environ. Saf.* 207, 111483.
- Lafi, W.K., Al-Qodah, Z., 2006. Combined advanced oxidation and biological treatment processes for the removal of pesticides from aqueous solutions. *J. Hazard. Mater.* 137, 489–497.
- Lage, A.L.A., Ribeiro, J.M., de Souza-Fagundes, E.M., Brugnera, M. F., da Silva Martins, D.C., 2019. Efficient atrazine degradation catalyzed by manganese porphyrins: determination of atrazine degradation products and their toxicity evaluation by human blood cells test models. *J. Hazard. Mater.* 378, 120748.
- Li, W., Zhao, Y., Yan, X., Duan, J., Saint, C.P., Beecham, S., 2019. Transformation pathway and toxicity assessment of malathion in aqueous solution during UV photolysis and photocatalysis. *Chemosphere* 234, 204–214.
- Liu, H., Guo, D., Feng, X., 2021. Plasma degradation of pesticides on the surface of corn and evaluation of its quality changes. *Sustainability* 13, 8830.
- Luguya, R., Jaquinod, L., Fronczek, F.R., Vicente, M.G.H., Smith, K. M., 2004. Synthesis and reactions of meso-(p-nitrophenyl) porphyrins. *Tetrahedron* 60, 2757–2763.
- Malakootian, M., Shahesmaeili, A., Faraji, M., Amiri, H., Martinez, S.S., 2020. Advanced oxidation processes for the removal of organophosphorus pesticides in aqueous matrices: a systematic review and meta-analysis. *Process Saf. Environ. Prot.* 134, 292–307.
- Martins, D.C. da S., Resende, I.T., da Silva, B.J.R., 2022. Degradation features of pesticides: a review on (metallo) porphyrin-mediated catalytic processes. *Environmental Science and Pollution Research* 29, 42384–42403.
- Moriya, M., Ohta, T., Watanabe, K., Miyazawa, T., Kato, K., Shirasu, Y., 1983. Further mutagenicity studies on pesticides in bacterial reversion assay systems. *Mutat. Res./Genet. Toxicol.* 116, 185–216.
- Pandiselvam, R., Kaavya, R., Jayanath, Y., Veenuttranon, K., Lueprasitsakul, P., Divya, V., Kothakota, A., Ramesh, S.V., 2020. Ozone as a novel emerging technology for the dissipation of pesticide residues in foods—a review. *Trends Food Sci. Technol.* 97, 38–54.
- Parida, V.K., Saidulu, D., Majumder, A., Srivastava, A., Gupta, B., Gupta, A.K., 2021. Emerging contaminants in wastewater: a critical review on occurrence, existing legislations, risk assessment, and sustainable treatment alternatives. *J. Environ. Chem. Eng.* 9, 105966.
- Pérez, M.H., Peñuela, G., Maldonado, M.I., Malato, O., Fernández-Ibáñez, P., Oller, I., Gernjak, W., Malato, S., 2006. Degradation of pesticides in water using solar advanced oxidation processes. *Appl. Catal. B: Environ.* 64, 272–281.
- Procter, M., Stochel, G., van Eldik, R., 2016. Spectroscopic and kinetic evidence for redox cycling, catalase and degradation activities of Mn III (TPPS) in a basic aqueous peroxide medium. *Chem. Commun.* 52, 5297–5300.
- Procter, M., Orzel, Ł., Stochel, G., van Eldik, R., 2020. A kinetic study on the efficient formation of high-valent Mn (TPPS)-oxo complexes by various oxidants. *Catalysts* 10, 610.
- Rajagopalan, V., Venkataraman, S., Rajendran, D.S., Kumar, V.V., Kumar, V.V., Rangasamy, G., 2023. Acetylcholinesterase biosensors for electrochemical detection of neurotoxic pesticides and

- acetylcholine neurotransmitter: a literature review. *Environ. Res.*, 227–115724
- Rebello, S.L.H., Pereira, M.M., Monsanto, P.V., Burrows, H.D., 2009. Catalytic oxidative degradation of s-triazine and phenoxyalkanoic acid based herbicides with metalloporphyrins and hydrogen peroxide: identification of two distinct reaction schemes. *J. Mol. Catal. A Chem.* 297, 35–43.
- Saha, T.K., Frauendorf, H., John, M., Dechert, S., Meyer, F., 2013. Efficient oxidative degradation of azo dyes by a water-soluble manganese porphyrin catalyst. *ChemCatChem* 5, 796–805.
- Sarangapani, C., Misra, N.N., Milosavljevic, V., Bourke, P., O'Regan, F., Cullen, P.J., 2016. Pesticide degradation in water using atmospheric air cold plasma. *J. Water Process Eng.* 9, 225–232.
- Silva, M., Azenha, M.E., Pereira, M.M., Burrows, H.D., Sarakha, M., Forano, C., Ribeiro, M.F., Fernandes, A., 2010. Immobilization of halogenated porphyrins and their copper complexes in MCM-41: environmentally friendly photocatalysts for the degradation of pesticides. *Appl. Catal. B: Environ.* 100, 1–9.
- Strotmann, U.J., Eglsaer, H., 1995. The toxicity of substituted phenols in the nitrification inhibition test and luminescent bacteria test. *Ecotoxicol. Environ. Saf.* 30, 269–273.
- Tony, A.M., El-Geundi, M.S., Hussein, S.M., Abdelwahab, M.Z., 2017. Degradation of malathion in aqueous solutions using advanced oxidation processes and chemical oxidation. *Direct Res. J. Agric. Food Sci.* 5, 174–185.
- Trocha, A., Impert, O., Katafias, A., van Eldik, R., 2021. Mechanistic details of the catalytic degradation of methylene blue by hydrogen peroxide in basic solution. the unexpected innocence of percarbonate. *Polyhedron* 210, 115507.
- Vormeier, P., Liebmann, L., Weisner, O., Liess, M., 2023. Width of vegetated buffer strips to protect aquatic life from pesticide effects. *Water Res.*, 119627
- Wang, T., Yu, C., Chu, Q., Wang, F., Lan, T., Wang, J., 2020. Adsorption behavior and mechanism of five pesticides on microplastics from agricultural polyethylene films. *Chemosphere* 244, 125491.
- Wang, M., Zhang, Y., Yu, G., Zhao, J., Chen, X., Yan, F., Li, J., Yin, Z., He, B., 2020. Monolayer porphyrin assembled SPS/PES membrane reactor for degradation of dyes under visible light irradiation coupling with continuous filtration. *J. Taiwan Inst. Chem. Eng.* 109, 62–70.
- Zaller, J.G., Kruse-Plab, M., Schlechtriemen, U., Gruber, E., Peer, M., Nadeem, I., Formayer, H., Hutter, H.-P., Landler, L., 2022. Pesticides in ambient air, influenced by surrounding land use and weather, pose a potential threat to biodiversity and humans. *Sci. Total Environ.* 838, 156012.
- Zhang, H., Li, Q., Li, B., Weng, B., Tian, Z., Yang, J., Hofkens, J., Lai, F., Liu, T., 2022. Atomically dispersed Pt sites on porous metal-organic frameworks to enable dual reaction mechanisms for enhanced photocatalytic hydrogen conversion. *J. Catal.* 407, 1–9.